Published in final edited form as:
Stroke. 2014 February ; 45(2): 473–478. doi:10.1161/STROKEAHA.113.003454.

Carotid Bifurcation Geometry is an Independent Predictor of Early Wall Thickening at the Carotid Bulb

Payam B. Bijari, PhD[1], **Bruce A. Wasserman, MD**[2], and **David A. Steinman, PhD**[1,*]

[1]Biomedical Simulation Laboratory, Department of Mechanical & Industrial Engineering and Institute of Biomaterials and Biomedical Engineering, University of Toronto, Toronto, Ontario, Canada

[2]Russell H. Morgan Department of Radiology and Radiological Sciences, Johns Hopkins University School of Medicine, Baltimore, Maryland, USA

Abstract

Background and Purpose—Lumen geometry has long been suspected as a risk factor for atherosclerosis by virtue of its influence on blood flow disturbances. Confirmation of this geometric risk hypothesis has, however, proved challenging owing to possible effects of wall thickening on geometry, and unproven links between candidate geometric variables and disturbed flow. The purpose of this study was to overcome these challenges.

Methods—The study relied on imaging and risk factor data from progressively refined subsets of the Atherosclerosis Risk in Communities (ARIC) Carotid MRI study. Group 1 (N=467) included only non-stenotic cases having sufficient-quality angiography for 3D analysis. Group 2 (N=346) excluded cases from Group 1 having common and internal carotid artery (ICA) wall thickness above previously-identified thresholds for inward remodeling. Group 3 (N=294) excluded cases from Group 2 having lumen irregularities, and thus was least likely to include lumen geometries influenced by wall thickening.

Results—Multiple linear regressions showed that for Group 3 bifurcation flare and proximal curvature were independent predictors of ICA wall thickness, consistent with their previously-demonstrated roles in predicting disturbed flow. For the broadest Group 1, flare was an independent predictor of ICA wall thickness, but with a sign change in regression coefficient reflecting effects of wall thickening on lumen geometry.

Conclusion—Carotid bifurcation geometry is an independent, albeit weak, predictor of its early wall thickening, but only when assumptions about geometric factors, and the influence of disease on them, are confronted. This highlights pitfalls of previous attempts to confirm geometric risk of atherosclerosis.

Keywords

Atherosclerosis; Carotid Artery; Geometry; MRI; Wall Shear Stress

[*]Corresponding author: steinman@mie.utoronto.ca; 416-978-7781(tel)/7753(fax).

DISCLOSURES

None.

Atherosclerosis develops primarily at bends and major branches of the arterial network, such as the carotid bifurcation.[1] This focal nature is inconsistent with the systemic nature of known cardiovascular risk factors. Decades of investigations have established that these atherogenic regions experience “disturbed” flow, characterized by low and oscillatory wall shear stress (WSS), which can induce endothelial dysfunction and subsequent increased LDL uptake.[2] Despite strong pathophysiological and experimental evidence that knowledge of disturbed blood flow dynamics might augment widely accepted systemic markers of atherosclerosis risk, clinical utility of such “local” risk factors remains unclear, owing to practical challenges of carrying out large-enough clinical studies via state-of the-art imaging and/or computational methods.[3, 4]

Instead it has been suggested, at least as far back as the early 1980s, that aspects of artery geometry (the primary determinant of local hemodynamics) might serve as clinically feasible surrogate local risk markers for atherosclerosis.[5] Early investigations of this geometric risk hypothesis were equivocal,[6–8] in part owing to relatively small sample sizes. Since the early 2000s, larger studies have reinvigorated the search for geometric risk factors for atherosclerosis. Analysis of nearly 3000 angiograms from the European Carotid Stenosis Trial confirmed the presence of major variations in carotid bifurcation geometry,[9] a necessary condition for geometric risk. In a community-based study of more than 3000 middle-aged adults, Polak et al.[10] found that traditional risk factors explained more variability of intima-media thickness (IMT) at the common carotid artery (CCA) than at the internal carotid artery (ICA) or carotid bulb. They hypothesized that these segment-specific differences were “likely linked to bifurcation geometry and differences in hemodynamics”. In an ultrasound study of 1300 normal, middle-aged-to-older adults, Sitzer et al.[11] demonstrated that orientation of the bifurcation within the neck was an independent predictor of high IMT at the carotid bulb. Most recently, a CT-based study of 178 older adults identified proximal ICA radius and ICA angle as significant independent predictors of stenosis.[12]

Common to these and other cross-sectional studies is the assumption that secondary effects of wall thickening on geometry can be ignored, or at least minimized by focusing on cases with mild (e.g., <30% NASCET) stenosis. As Thomas et al.[13] demonstrated, however, there is significantly wider variability of the carotid bifurcation geometry of older adults with mild or no disease compared to young, nominally healthy adults. Most studies also assume that their candidate geometric risk factors are predictors of disturbed WSS, which provides the essential mechanistic link between geometry and early wall thickening. As Lee et al.[14] demonstrated, however, that may not always be the case. The aim of the present study was therefore to test the geometric risk hypothesis in a way that, for the first time, explicitly accounts for the above assumptions. Specifically, we hypothesized that variables characterizing carotid bifurcation geometry are independent predictors of wall thickening at the ICA, but not the CCA; but that this will only be evident if those geometric variables are proven predictors of disturbed WSS, and then only if effects of wall thickening on carotid bifurcation geometry are carefully excluded.

MATERIALS AND METHODS

Study participants and imaging protocols

This study focused on MRI and cardiovascular risk factor data collected by the Atherosclerosis Risk in Communities (ARIC) Carotid MRI study.[15] That study enrolled 2066 participants, aged 60–85 years, to investigate genomic, metabolic, and cellular correlates of carotid plaque components. Informed consent was obtained from all participants and local institutional review committees approved the study.

A comprehensive 1.5T MRI protocol was used for all participants, as detailed by Wasserman et al.[15] Of relevance to the present study, a 3D time-of-flight MRA was acquired to localize the bifurcations and measure NASCET stenosis severity. Individual T1-weighted black blood MRI slices were acquired at each CCA 1.5 cm below the bifurcation flow divider. A series of 16 black blood images was then acquired through the carotid bifurcation having the greater maximum IMT at the participant's most recent ARIC ultrasound scan, or the contralateral carotid if its wall appeared thicker or its lumen more stenotic. A 3D contrast-enhanced MRA was then acquired during intravenous injection of gadodiamide. Five minutes after this injection, the black blood acquisitions were repeated.

Analysis of carotid wall thickness

Post-contrast black blood images were previously analyzed using semi-automated software as part of the ARIC Carotid MRI study.[15] Contours were drawn to delineate the lumen and outer wall in each image. The arterial wall was then automatically divided into 12 radial segments, and a wall thickness was measured for each. Mean and maximum wall thicknesses were reported for both CCAs, and for the selected ICA at the first black blood slice distal to the flow divider, a standard location referred to as FD+1. In some cases, the carotid plaque of interest was located far above the flow divider, and so the FD+1 location was not included in the black blood series. As a result, ICA wall thickness data at FD+1 were available only for N=1064 ICAs,[16] which is the cohort from which our study groups were defined by applying increasingly stringent exclusion criteria to progressively filter out those cases that were likely to include an effect of wall thickening on lumen geometry.

Study groups and exclusion criteria

Since presence of a stenosis implies inward remodeling, and thus possible effects of wall thickening on lumen geometry, we first excluded 462 of the 1064 cases having >0% NASCET stenosis. From these we excluded 60 cases having incomplete risk factor data, and 75 cases that could not be segmented reliably from the contrast-enhanced MRA owing to weak arterial signal or poor venous suppression. Per Table 1, the remaining 467 cases were the starting point for the present study, and are denoted **Group 1**.

Since a 0% NASCET stenosis cannot alone exclude the possibility of inward remodeling, a more restricted **Group 2** was defined by further excluding 121 cases with ICA wall thickness>1.38 mm and CCA wall thickness>2.06 mm, previously identified as thresholds for inward remodeling in this ARIC Carotid MRI cohort.[16] These thresholds could, however, only be applied at the two slices where wall thickness was measured. To minimize

the possibility of inward remodeling elsewhere at the bifurcation, we defined an even more restricted **Group 3** by further excluding 52 cases with lumen shape irregularities or apparent stenosis proximal to the bifurcation, based on inspection of the segmented surfaces by an operator blinded to the wall thickness measurements.

Lumen segmentation and geometric analysis

Each of the 467 carotid bifurcations from Group 1 was digitally segmented from the contrast-enhanced MRA using a 3D level set approach. As shown in Figure 1 for representative cases, centerlines were then generated along the ICA-CCA and ECA-CCA tracts. As introduced by Thomas et al.,[13] these centerlines and their associated maximally-inscribed spheres can be used to define a natural coordinate system for each bifurcation, allowing lumen cross-sections to be extracted at standardized locations. These elements form the basis for calculating the geometric variables described below. All analyses were automated using customized software (AriX 1.1, Orobix Srl, Bergamo, Italy), based on methods previously developed using the open-source Vascular Modelling ToolKit,[17] and shown to be highly reproducible.[18]

Geometric variables

In 2008, Lee et al.[14] identified bifurcation area ratio and ICA-CCA tortuosity as significant predictors of low and oscillatory WSS at the carotid bifurcation. Per Figure 1, they defined "**Area Ratio**" (AR1 in Lee et al.[14]) as the sum of the cross-sectional areas located one sphere radius distal to the bifurcation origin (ICA1 and ECA1 in Figure 1) divided by the area of the CCA section three radii proximal to the bifurcation (CCA3 in Figure 1). "**Tortuosity**" was defined as the length of the centerline between CCA3 and the distal ICA (ICA5 in Figure 1), divided by the straight-line distance between these points.

Recently, Bijari et al.[19] demonstrated that "hemodynamically-inspired" redefinitions of Lee et al.'s geometric variables could substantially improve their ability to predict the burden of disturbed WSS. Specifically, per Figure 1, "**Flare**" (FlareA in Bijari et al.[19]) was defined as the maximum bifurcation cross-sectional area (CCAmax in Figure 1) divided by the area of the CCA3 section. "**Curvature**" (Tort2D in Bijari et al.[19]) was defined similarly to Lee et al.'s tortuosity, but excluding the downstream (ICA) segment and projecting the retained (CCA) segment onto a 2D plane.

Physically, flaring (i.e., expansion) of the lumen promotes flow separation and consequent low and oscillatory WSS. On the other hand, curvature of the CCA proximal to the bifurcation induces swirling flow, which *suppresses* flow separation.[20] As a result, per Figure 1, bifurcations with high flare and low curvature are at highest risk of disturbed WSS, whereas low flare and high curvature are at lowest risk.

Cardiovascular risk factors

Systemic risk factors used in the present study corresponded to those included by Polak et al.,[10] and were determined previously by the ARIC Carotid MRI study.[16] In that study, centrally trained staff measured blood pressure, height and weight. Body mass index (BMI) was calculated as weight in kilograms divided by the square of height in meters. Smoking

status was assessed using a standardized questionnaire. Diabetes was defined as fasting blood glucose ≥126 mg/dL or taking insulin and/or oral hypoglycemic agents. Both fasting glucose and fasting lipid profile (triglycerides, total cholesterol, and HDL cholesterol) were measured using standard laboratory techniques. LDL cholesterol was estimated using the Friedewald approximation. Hypertension was defined as seated resting systolic blood pressure >140 mmHg or diastolic blood pressure >90 mmHg or history of taking antihypertensive medications. Descriptive statistics for cardiovascular risk factors are summarized in Table 2. For continuous variables, t-tests revealed no significant differences between the original N=1064 cohort and any of three groups used in the present study.

Statistical analysis

Multiple linear regressions were performed to determine whether either of the candidate geometric variable pairs (Flare & Curvature; Area Ratio & Tortuosity) could, independently of the above-described cardiovascular risk factors, significantly predict maximum ICA wall thickness (ICA-WT) or mean CCA wall thickness (CCA-WT). All variables were standardized, and variance inflation factors were calculated to avoid multicollinearity in the predictor variables, with a threshold of 5. Quantile-quantile plots and Shapiro-Wilk tests were used to assess the normality of the residuals. Regression coefficients having $P<0.05$ were considered significant. All analyses were performed using SPSS Version 17.0.1 (IBM Corporation, Armonk, NY).

RESULTS

Starting with the broadest Group 1, Table 3 shows that Flare, but not Curvature, was a significant independent predictor of ICA-WT. The negative regression coefficient ($\beta= -0.199$, $p<0.001$) implies that thicker walls were associated with narrower lumens, which would be expected if there was inward remodeling. Indeed, after explicitly excluding inward remodeling (Group 2), Flare no longer predicted ICA-WT. After further excluding other cases where wall thickening may have affected geometry (Group 3), both Flare ($\beta=0.173$, $p=0.013$) and Curvature ($\beta= -0.135$, $p=0.047$) emerged as significant, albeit weak, independent predictors of ICA-WT, with opposite signs consistent with their roles in promoting vs. suppressing disturbed flow.[20]

On the other hand, as shown in Table 4, neither Area Ratio nor Tortuosity were significant predictors of ICA-WT for Group 3, consistent with these two variables being weaker predictors of disturbed WSS compared to their “hemodynamically-inspired” counterparts Flare and Curvature. For Group 1, however, Area Ratio, like Flare, was negatively associated with ICA-WT ($\beta= -0.213$, $p<0.001$) again suggesting a possible effect of inward remodeling on geometry.

Turning attention to the proximal CCA, Table 3 shows that both Flare ($\beta= -0.137$, $p=0.012$) and Curvature ($\beta= -0.113$, $p=0.033$) were independent predictors of CCA-WT for the broadest Group 1, with the negative Flare coefficient again suggesting effects of inward remodeling. This inverse association persisted into Group 2 ($\beta= -0.148$, $p=0.025$). For the most restricted Group 3, however, neither Flare nor Curvature predicted CCA-WT, consistent with the CCA being a site of relatively undisturbed WSS.

DISCUSSION

Geometric factors representing carotid bifurcation lumen expansion ("Flare") and proximal curvature ("Curvature") have previously been shown to be strong and significant predictors of flow disturbances at the carotid bifurcation.[19] They are now shown to be independent, albeit weak, predictors of ICA-WT. Moreover, the signs of the respective regression coefficients naturally uncovered the competing physical effects of flare and curvature on flow disturbances. Furthermore, neither geometric variable predicted CCA-WT, where blood flow is expected to be undisturbed. This reflects the "segment-specific" influence of hemodynamics on carotid wall thickness.[10] Although wall thickening does not always imply atherosclerosis, these findings are consistent with the geometric risk hypothesis of atherosclerosis, which is predicated on the link between low and oscillatory WSS and early wall thickening at the carotid bulb.[21]

Another key finding was that, when stenosis severity alone was used to exclude secondary effects of wall thickening on lumen geometry, geometric risk factor associations were altered in a way no longer consistent with the role of geometry in promoting or suppressing disturbed WSS. Only after excluding cases with inward remodeling and lumen irregularities – in other words, systematically narrowing the focus to cases at the earliest stages of wall thickening – were our findings in line with the geometric risk hypothesis. Finally, we showed that associations between geometry and wall thickness could be masked using geometric variables (Area Ratio and Tortuosity) that were previously shown to be weaker predictors of disturbed WSS. As discussed below, these findings have implications for conclusions drawn from previous tests of the geometric risk hypothesis.

Relationship to Previous Studies

Recently, Phan et al.[12] reported that radius and angulation of the ICA at the carotid bifurcation were significantly and independently associated with stenosis severity in a CT-based study that included cases with stenosis severities up to >90%. From this they concluded that those geometric factors "may enhance the risk of stenosis independent of traditional vascular risk factors". Regarding possible effects of stenosis on geometry, the authors implied that these were minimized because they used "different methods to measure the minimum ICA radius and the ICA radius at the bifurcation." To demonstrate that this was probably not the case, we repeated our multiple regressions using the mean radius of the cross-section at location ICA1 (Figure 1) and ICA-CCA angle, variables comparable to Phan et al.'s ICA radius and angulation, respectively. As was the case for our Area Ratio, we found a significant inverse association between ICA1 radius and ICA-WT for Group 1 ($\beta = -0.168$, $p=0.002$) – consistent with Phan et al. and thus inconsistent with the physical effect of lumen expansion on disturbed WSS – but not for Group 3. ICA-CCA angle was not associated with ICA-WT for any groups. It is therefore doubtful that Phan et al.'s variables may, as they suggested, "be of help in *very early* [our italics] identification of patients at high risk of developing carotid artery atherosclerosis." Instead, their associations are much more likely a *consequence* rather than a *cause* of stenosis development, highlighting the sensitivity of geometric risk factor associations to the choice of exclusion criteria.

In an earlier ultrasound-based study of normal individuals aged 40–70 years, Sitzer et al.[11] found a higher prevalence of dorsal/dorsomedial ICA origin (i.e., rotation of the carotid bifurcation within the neck) for cases with highest ICA bulb IMT, even after controlling for cardiovascular risk factors. From this they concluded "angle of ICA origin may be an independent risk factor for early atherosclerotic changes at the ICA bulb". On the other hand, ICA angle of origin was previously shown to be significantly less variable in young adults vs. older adults with mild disease,[22] suggesting that such rotation may simply be a consequence rather than a cause of vascular aging. This is because there is no obvious relationship between rotation of the carotid bifurcation and flow disturbances *within* the carotid bifurcation. Sitzer et al. did attempt to provide such a mechanistic link by suggesting that their angle of ICA origin may be related to the "ICA angle of insertion" (comparable to Lee et al.'s[14] ICA-CCA angle), which *has* been linked to flow disturbances; however, it is not clear how or if rotation of the carotid bifurcation systematically alters ICA angle of insertion. Instead, consider that systemic factors like hypertension can cause arterial remodeling, and such remodeling is known to increase arterial tortuosity.[23] Thus it is plausible that the carotid bifurcation, which is not fixed within the carotid sheath, may rotate under distal or proximal tortuosity. Thus, unlike the present study, there is no clear mechanistic path from geometric risk factor to the wall response it purports to predict.

Potential Limitations and Implications

Although our "hemodynamically-inspired" geometric variables were found to be significant independent predictors of ICA-WT, their inclusion served to increase R^2 from 0.112 to only 0.135 (Table 3). A much larger increase in R^2 was not, however, expected as Polak et al.[10] showed that prediction of IMT by conventional cardiovascular risk factors resulted in R^2=0.112 for the carotid bulb and R^2=0.268 for the CCA. This difference in R^2, which they attributed to "unknown hemodynamic or geometric factors", would seem to place an upper bound on the influence of geometric risk vs. conventional risk factors. Nevertheless, the muted impact of geometry in the present study may also reflect several potential limitations of our study design. First, our geometric variables are strong, but not perfect, predictors of disturbed WSS. They might therefore mask a stronger relationship between disturbed WSS and ICA wall thickening. Second, ICA-WT was measured at a location slightly distal to the flow divider (i.e., FD+1), whereas Lee et al.[14] have shown the disturbed WSS tends to be concentrated at the carotid bulb *proximal* to the flow divider. Thus, measurement of wall thickness there might result in stronger associations. Third, it is difficult to justify a large, prospective study of geometric risk in young adults, and so our study was relatively small, retrospective, and focused on older adults.

It should also be noted that our study was not intended to be an epidemiological study, and therefore our groups do not necessarily represent the characteristics of the general population. For example, the narrow age range of ARIC participants (71.1± 5.5 years) and larger proportion of hypertensives (~70%, vs. 22% for Polak et al.[10]) likely served to mask the well-known association between wall thickening and aging or systolic BP, respectively. On the other hand, race and sex, the other predominant predictors of carotid IMT identified by Polak et al., were both significant predictors of ICA-WT in our study.

Notwithstanding the above potential limitations, Polak et al.[10] appear to set a modest upper bound on the influence of local vs. known or unknown systemic cardiovascular risk factors on wall thickening. Thus, while our findings appear to prove the *principle* that carotid bifurcation geometry (and, by extension, local hemodynamics) can indeed be considered a risk factor for early carotid wall thickening, in the spirit of Hlatky et al.,[24] its incremental value, clinical utility and, ultimately, cost-effectiveness as a risk marker for atherosclerosis appears questionable.

Acknowledgments

FUNDING SOURCES

This study was supported by Canadian Institutes of Health Research grant MOP-62934, to DAS. DAS was supported by a Heart & Stroke Foundation Career Investigator award. The Atherosclerosis Risk in Communities Study is carried out as a collaborative study supported by National Heart, Lung, and Blood Institute contracts (HHSN268201100005C, HHSN268201100006C, HHSN268201100007C, HHSN268201100008C, HHSN268201100009C, HHSN268201100010C, HHSN268201100011C, and HHSN268201100012C) with the ARIC Carotid MRI examination funded by U01HL075572-01.

The authors thank the staff and participants of the ARIC study for their important contributions.

References

1. DeBakey ME, Lawrie GM, Glaeser DH. Patterns of atherosclerosis and their surgical significance. Ann Surg. 1985; 201:115–131. [PubMed: 3155934]
2. Davies PF. Hemodynamic shear stress and the endothelium in cardiovascular pathophysiology. Nat Clin Pract Cardiovasc Med. 2009; 6:16–26. [PubMed: 19029993]
3. Markl M, Wegent F, Zech T, Bauer S, Strecker C, Schumacher M, et al. In vivo wall shear stress distribution in the carotid artery: Effect of bifurcation geometry, internal carotid artery stenosis, and recanalization therapy. Circ Cardiovasc Imaging. 2010; 3:647–655. [PubMed: 20847189]
4. Taylor CA, Steinman DA. Image-based modeling of blood flow and vessel wall dynamics: Applications, methods and future directions. Ann Biomed Eng. 2010; 38:1188–1203. [PubMed: 20087775]
5. Friedman MH, Deters OJ, Mark FF, Bargeron CB, Hutchins GM. Arterial geometry affects hemodynamics. A potential risk factor for atherosclerosis. Atherosclerosis. 1983; 46:225–231. [PubMed: 6838702]
6. Harrison MJG, Marshall J. Does the geometry of the carotid bifurcation affect its predisposition to atheroma? Stroke. 1983; 14:117–118. [PubMed: 6823681]
7. Fisher M, Fieman S. Geometric factors of the bifurcation in carotid atherogenesis. Stroke. 1990; 21:267–271. [PubMed: 2305402]
8. Spelde AG, de Vos RA, Hoogendam IJ, Heethaar RM. Pathological-anatomical study concerning the geometry and atherosclerosis of the carotid bifurcation. Eur J Vasc Surg. 1990; 4:345–348. [PubMed: 2397771]
9. Schulz UG, Rothwell PM. Major variation in carotid bifurcation anatomy: A possible risk factor for plaque development? Stroke. 2001; 32:2522–2529. [PubMed: 11692011]
10. Polak J, Person S, Wei G, Godreau A, Jacobs D, Harrington A, et al. Segment-specific associations of carotid intima-media thickness with cardiovascular risk factors: The coronary artery risk development in young adults (CARDIA) study. Stroke. 2010; 41:9–15. [PubMed: 19910544]
11. Sitzer M, Puac D, Buehler A, Steckel DA, Von Kegler S, Markus HS, et al. Internal carotid artery angle of origin: A novel risk factor for early carotid atherosclerosis. Stroke. 2003; 34:950–955. [PubMed: 12637694]
12. Phan TG, Beare RJ, Jolley D, Das G, Ren M, Wong K, et al. Carotid artery anatomy and geometry as risk factors for carotid atherosclerotic disease. Stroke. 2012; 43:1596–1601. [PubMed: 22511010]

13. Thomas JB, Antiga L, Che SL, Milner JS, Hangan-Steinman DA, Spence JD, et al. Variation in the carotid bifurcation geometry of young versus older adults: Implications for geometric risk of atherosclerosis. Stroke. 2005; 36:2450–2456. [PubMed: 16224089]

14. Lee SW, Antiga L, Spence JD, Steinman DA. Geometry of the carotid bifurcation predicts its exposure to disturbed flow. Stroke. 2008; 39:2341–2347. [PubMed: 18556585]

15. Wasserman BA, Astor BC, Sharrett AR, Swingen C, Catellier D. MRI measurements of carotid plaque in the atherosclerosis risk in communities (ARIC) study: Methods, reliability and descriptive statistics. J Magn Reson Imaging. 2010; 31:406–415. [PubMed: 20099354]

16. Astor BC, Sharrett AR, Coresh J, Chambless LE, Wasserman BA. Remodeling of carotid arteries detected with MR imaging: Atherosclerosis risk in communities carotid MRI study. Radiology. 2010; 256:879–886. [PubMed: 20651061]

17. Antiga L, Piccinelli M, Botti L, Ene-Iordache B, Remuzzi A, Steinman DA. An image-based modeling framework for patient-specific computational hemodynamics. Med Biol Eng Comput. 2008; 46:1097–1112. [PubMed: 19002516]

18. Bijari PB, Antiga L, Wasserman BA, Steinman DA. Scan-rescan reproducibility of carotid bifurcation geometry from routine contrast-enhanced MR angiography. J Magn Reson Imaging. 2011; 33:482–489. [PubMed: 21274992]

19. Bijari PB, Antiga L, Gallo D, Wasserman BA, Steinman DA. Improved prediction of disturbed flow via hemodynamically-inspired geometric variables. J Biomech. 2012; 45:1632–1637. [PubMed: 22552156]

20. Zhang Q, Steinman DA, Friedman MH. Use of factor analysis to characterize arterial geometry and predict hemodynamic risk: Application to the human carotid bifurcation. J Biomech Eng. 2010; 132:114505. [PubMed: 21034157]

21. Ku DN, Giddens DP, Zarins CK, Glagov S. Pulsatile flow and atherosclerosis in the human carotid bifurcation. Positive correlation between plaque location and low oscillating shear stress. Arteriosclerosis. 1985; 5:293–302. [PubMed: 3994585]

22. Thomas JB, Jong L, Spence JD, Wasserman BA, Rutt BK, Steinman DA. Anthropometric data for magnetic resonance imaging of the carotid bifurcation. J Magn Reson Imaging. 2005; 21:845–849. [PubMed: 15906347]

23. Jackson ZS, Gotlieb AI, Langille BL. Wall tissue remodeling regulates longitudinal tension in arteries. Circ Res. 2002; 90:918–925. [PubMed: 11988494]

24. Hlatky MA, Greenland P, Arnett DK, Ballantyne CM, Criqui MH, Elkind MS, et al. Criteria for evaluation of novel markers of cardiovascular risk: A scientific statement from the american heart association. Circulation. 2009; 119:2408–2416. [PubMed: 19364974]

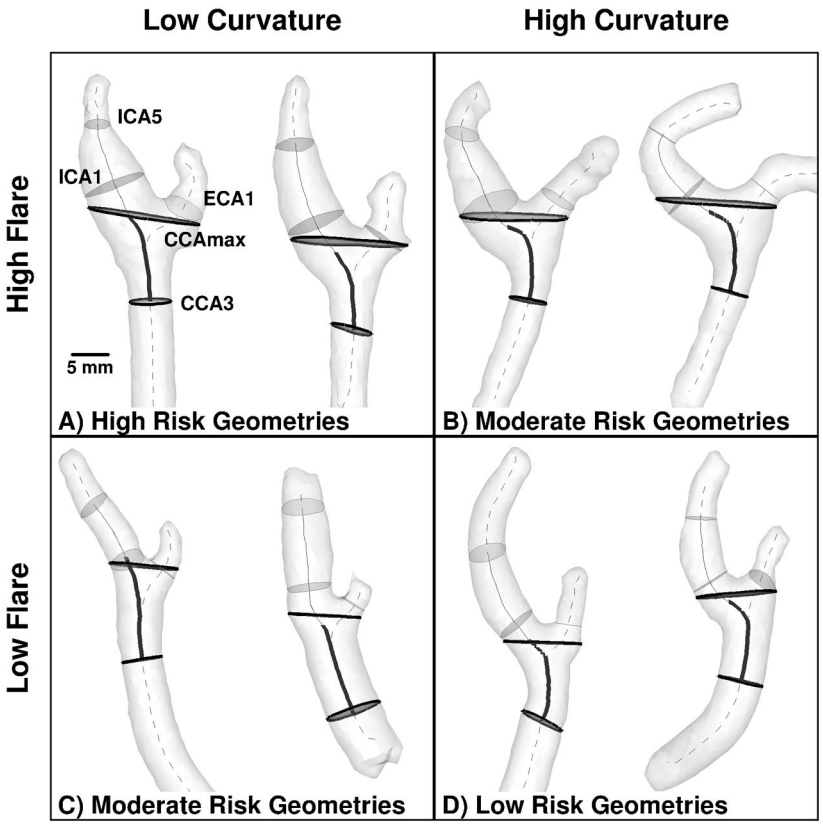

Figure 1.

Representative cases having extreme values of Flare and Curvature, indicating which combinations are expected to elicit high, moderate and low risk of disturbed wall shear stress. Thicker and/or darker cross-sections and centerline segments are those used to compute Flare and Curvature, respectively, as detailed in the Methods. Thinner and/or lighter elements are those used to compute Area Ratio and Tortuosity.

Table 1

Summary of exclusion criteria and study groups

Cases	Description
1064	ARIC Carotid MRI remodeling study cohort[16]
−462	NASCET stenosis >0%
−60	Incomplete cardiovascular risk factor data
−75	Low quality contrast-enhanced MRA
467	**Group 1: no stenosis (0% NASCET stenosis)**
−121	ICA-WT >1.38 mm or CCA-WT >2.06 mm
346	**Group 2: no stenosis, no inward remodelling**
−52	Irregular lumen shape or apparent stenosis
294	**Group 3 no-stenosis, no inward remodeling, no lumen irregularity**

Table 2

Descriptive statistics for cardiovascular risk factors for each group.

Cardiovascular Risk Factors*	Astor et al.[16] (N=1064)	Group 1 (N=467)	Group 2 (N=346)	Group 3 (N=294)
Age (years)	71.1±5.5	70.1±5.5	70.1±5.7	70.0±5.5
Female (%)	51.1	52.7	56.6	55.0
Black (%)	19.2	21.0	23.7	22.1
Systolic BP (mmHg)	123.9±14.1	122.2±13.8	122.5±14.4	122.0±14.1
Diastolic BP (mmHg)	70.0±7.8	70.4±7.9	70.4±8.1	70.5±8.1
Hypertension (%)	73.2	68.3	67.0	65.3
Triglycerides (mg/dL)	138.3±64.3	131.2±58.3	129.8±58.1	129.7±60.1
LDL Cholesterol (mg/dL)	124.2±25.0	121.8±25.2	121.3±26.8	119.0±26.6
HDL Cholesterol (mg/dL)	50.5±15.2	51.8±15.3	52.6±15.6	52.4±15.6
Diabetes (%)	26.0	22.7	21.4	21.8
Glucose (mg/dL)	106.6±22.9	106.0±23.6	105.6±23.9	106.2±25.9
BMI (kg/m^2)	28.2±4.8	28.4±4.9	28.3±5.1	28.3±5.3
Ever smoker (%)	52.9	49.2	45.6	46.5

* For continuous variables, shown are means±stdevs

Table 3

Standardized coefficients (β) from multiple regressions of ICA-WT and CCA-WT with conventional cardiovascular risk factors and Bijari et al.'s[19] "hemodynamically-inspired" geometric variables as predictors.

	ICA-WT			CCA-WT		
Predictor	**Group 1**	**Group 2**	**Group 3**	**Group 1**	**Group 2**	**Group 3**
Flare	**−0.199*****	0.019	**0.173***	**−0.137***	**−0.148***	−0.076
Curvature	0.024	0.015	**−0.135***	**0.113***	0.072	0.071
Age	−0.074	−0.008	−0.052	0.029	0.064	0.056
Sex†	**0.142***	0.088	**0.160***	0.098	0.116	0.132
Race††	**0.125***			**0.150****	0.066	0.047
Systolic BP	−0.048	0.052	0.098	0.082	0.062	0.148
Diastolic BP	0.067	0.122	0.107	−0.011	0.046	−0.005
Hypertension	0.091	−0.004	0.040	**0.155****	0.095	0.106
Triglycerides	−0.073	0.066	0.077	−0.046	0.040	0.041
LDL Cholesterol	0.065	0.096	0.074	0.078	0.065	0.076
HDL Cholesterol	−0.046	0.019	0.097	0.070	**0.103***	**0.165***
Diabetes	0.061	−0.034	−0.076	−0.012	−0.087	−0.138
Glucose	0.017	0.064	0.107	0.022	0.060	0.063
BMI	−0.016	−0.050	−0.045	−0.064	−0.108†	−0.129
Ever Smoker	0.043	0.042	−0.011	**0.101***	0.064	0.017
Total Model R^2	0.099	0.082	0.135	0.106	0.095	0.113
CV Factor-only R^2	0.069	0.081	0.112	0.090	0.081	0.108

† Male=1, Female=0;

†† White=1, Black=0;

* p<0.05;

** p<0.01;

*** p<0.001

Table 4

Standardized coefficients (β) for geometric variables from multiple regressions of ICA-WT with conventional cardiovascular risk factors and Lee et al.'s[14] original geometric variables as predictors.

	ICA-WT		
Predictor	**Group 1**	**Group2**	**Group 3**
Area Ratio	**−0.213*****	−0.012	0.109
Tortuosity	0.071	0.112	0.015
Total Model R^2	0.107	0.091	0.123

* p<0.05;

** p<0.01;

*** p<0.001